 doi:10.20944/preprints201912.0191.v1

Classifying superconductivity in an infinite-layer nickelate $Nd_{0.8}Sr_{0.2}NiO_2$

E. F. Talantsev[1,2*]

[1]M.N. Mikheev Institute of Metal Physics, Ural Branch, Russian Academy of Sciences, 18, S. Kovalevskoy St., Ekaterinburg, 620108, Russia

[2]NANOTECH Centre, Ural Federal University, 19 Mira St., Ekaterinburg, 620002, Russia

[*]E-mail: evgeny.talantsev@imp.uran.ru

Abstract

Recently Li *et al* (2019 Nature **572** 624) discovered a new type of oxide superconductor $Nd_{0.8}Sr_{0.2}NiO_2$ with T_c = 14 K. To classify superconductivity in this infinite-layer nickelate experimental upper critical field, $B_{c2}(T)$, and the self-field critical current densities, $J_c(sf,T)$, reported by Li *et al* (2019 Nature **572** 624), are analysed in assumption of *s*-, *d*-, and *p*-wave pairing symmetries and single- and multiple-band superconductivity. Based on deduced the ground-state superconducting energy gap, $\Delta(0)$, the London penetration depth, $\lambda(0)$, the relative jump in electronic specific heat at T_c, $\Delta C/C$, and the ratio of $2\Delta(0)/k_BT_c$, we conclude that $Nd_{0.8}Sr_{0.2}NiO_2$ is type-II high-κ weak-coupled single-band *s*-wave superconductor.

Classifying superconductivity in an infinite-layer nickelate $Nd_{0.8}Sr_{0.2}NiO_2$

I. Introduction

For several decades the term of infinite-layer superconductor was referred to a copper-oxide superconducting compounds, $Sr_{1-x}M_xCuO_2$ (M=La, Nd, Ca, Sr…) [1,2], until recently, Li *et al* [3] have extended this class of unconventional superconductors by the discovery of superconductivity at T_c = 14 K in $Nd_{0.8}Sr_{0.2}NiO_2$ nickelate. Thus, bulk superconducting oxides family, i.e. tungsten bronzes [4], titanates [5], bismuthates [6], cuprates [7], and ruthenates [8] extends by a new nickelate member. Several research groups proposed different models for superconducting state in this compound [9-12], and the exhibiting of the superconducting state in this compound is in a debate [13].

In this paper, to classify superconductivity in this new class of oxide superconductors the temperature-dependent upper critical field, $B_{c2}(T)$, and the self-field critical current density, $J_c(sf,T)$, are analysed within *s*-, *d*-, and *p*-pairing symmetries. In result, it is shown that infinite-layer $Nd_{0.8}Sr_{0.2}NiO_2$ nickelate is weak-coupled single band *s*-wave superconductor.

II. Models description

The Ginzburg-Landau theory [14] has two fundamental lengths, one is the coherence length, $\xi(T)$, and the second is London penetration depth, $\lambda(T)$. The ground state coherence length, $\xi(0)$, is given by [14,15]:

$$B_{c2}(0) = \frac{\phi_0}{2 \cdot \pi \cdot \xi^2(0)}, \qquad (1)$$

where $\phi_0 = 2.068 \cdot 10^{-15}$ Wb is magnetic flux quantum, and $B_{c2}(0)$ is the ground state upper critical field. For temperature dependent coherence length, $\xi(T)$, several models were proposed [14,15-21]. In this paper, to deduce the ground state coherence length, $\xi(0)$, in infinite-layer $Nd_{0.8}Sr_{0.2}NiO_2$ nickelate superconductor, three models are used. The first model was proposed by Gor'kov [16,17] (Gor'kov model):

Preprints (www.preprints.org) | NOT PEER-REVIEWED | Posted: 15 December 2019 doi:10.20944/preprints201912.0191.v1

$$B_{c2}(T) = \frac{\phi_0}{2\cdot\pi\cdot\xi^2(0)} \cdot \left(\frac{1.77-0.43\cdot\left(\frac{T}{T_c}\right)^2+0.07\cdot\left(\frac{T}{T_c}\right)^4}{1.77}\right) \cdot \left[1-\left(\frac{T}{T_c}\right)^2\right]. \quad (2)$$

The second model was proposed by Baumgartner *et al* [20] (B-WHH):

$$B_{c2}(T) = \frac{\phi_0}{2\cdot\pi\cdot\xi^2(0)} \cdot \left(\frac{\left(1-\frac{T}{T_c}\right)-0.153\cdot\left(1-\frac{T}{T_c}\right)^2-0.152\cdot\left(1-\frac{T}{T_c}\right)^4}{0.693}\right) \quad (3)$$

And the third model was proposed recently in our recent report [21]:

$$B_{c2}(T) = \frac{\phi_0}{2\cdot\pi\cdot\xi^2(0)} \cdot \left[\left(\frac{1.77-0.43\cdot\left(\frac{T}{T_c}\right)^2+0.07\cdot\left(\frac{T}{T_c}\right)^4}{1.77}\right)^2 \cdot \frac{1}{1-\frac{1}{2\cdot k_B\cdot T}\cdot\int_0^\infty \frac{d\varepsilon}{cosh^2\left(\frac{\sqrt{\varepsilon^2+\Delta^2(T)}}{2\cdot k_B\cdot T}\right)}}\right] \quad (4)$$

where k_B is Boltzmann constant, and $\Delta(T)$ is the temperature-dependent superconducting gap, for which analytical expression was given by Gross *et al* [22]:

$$\Delta(T) = \Delta(0)\cdot tanh\left[\frac{\pi\cdot k_B\cdot T_c}{\Delta(0)}\cdot\sqrt{\eta\cdot\frac{\Delta C}{C}\cdot\left(\frac{T_c}{T}-1\right)}\right] \quad (5)$$

where $\Delta(0)$ is the ground state energy gap amplitude, $\Delta C/C$ is the relative jump in electronic specific heat at T_c, $\eta = 2/3$ for *s*-wave superconductors [22].

Thus, $\xi(0)$ and T_c can be obtained by fitting experimental $B_{c2}(T)$ data to Eqs. 2-4. In addition, $\Delta C/C$, $\Delta(0)$ and, thus, the ratio of $\frac{2\Delta(0)}{k_B T_c}$, can be deduced as free-fitting parameters by fitting experimental $B_{c2}(T)$ data to Eq. 4. More details about the procedures can be found elsewhere [23].

There is an alternative way to deduce $\Delta(0)$, $\Delta C/C$, T_c and $\frac{2\Delta(0)}{k_B T_c}$ by the fit of experimental self-field critical current density, $J_c(\mathrm{sf},T)$, to universal equation, which is for thin-film superconductors reduced to simple form [23,24]:

$$J_c(\mathrm{sf},T) = \frac{\phi_0}{4\pi\mu_0}\cdot\frac{ln\left(1+\sqrt{2}\cdot\frac{\lambda(0)}{\xi(0)}\right)}{\lambda^3(T)} \quad (6)$$

where $\phi_0 = 2.067\times10^{-15}$ Wb is the magnetic flux quantum, $\mu_0 = 4\pi\times10^{-7}$ H/m is the magnetic permeability of free space, and the London penetration depth, $\lambda(T)$, is given by:

1. $$\lambda(T) = \frac{\lambda(0)}{\sqrt{1-\frac{1}{2\cdot k_B\cdot T}\cdot\int_0^\infty \frac{d\varepsilon}{\cosh^2\left(\frac{\sqrt{\varepsilon^2+\Delta^2(T)}}{2\cdot k_B\cdot T}\right)}}}, \quad (7)$$

for *s*-wave superconductors, where Δ(*T*) is given by Eq. 5 [22,25].

2. $$\lambda(T) = \frac{\lambda(0)}{\sqrt{1-\frac{1}{2\cdot k_B\cdot T}\cdot\int_0^{2\pi} cos^2(\theta)\cdot\left(\int_0^\infty \frac{d\varepsilon}{cosh^2\left(\frac{\sqrt{\varepsilon^2+\Delta^2(T,\theta)}}{2\cdot k_B\cdot T}\right)}\right)\cdot d\theta}} \quad (8)$$

for *d*-wave superconductors, where the superconducting energy gap, Δ(*T*,*θ*), is given by [22,25]:

$$\Delta(T,\theta) = \Delta_m(T)\cdot cos(2\theta) \quad (9)$$

where $\Delta_m(T)$ is the is the maximum amplitude of the *k*-dependent *d*-wave gap given by Eq. 5, *θ* is the angle around the Fermi surface subtended at (*π*, *π*) in the Brillouin zone (details can be found elsewhere [22,25,26]). In Eq. 9 the value of $\eta = 7/5$ [22,25,26].

3. And *p*-wave symmetry [22,25], which only recently was tested to fit critical current densities in superconductors [22,25]:

$$\lambda_{(p,a)(\perp,\parallel)}(T) = \frac{\lambda_{(p,a)(\perp,\parallel)}(0)}{\sqrt{1-\frac{3}{4\cdot k_B\cdot T}\cdot\int_0^1 w_{\perp,\parallel}(x)\cdot\left(\int_0^\infty \frac{d\varepsilon}{cosh^2\left(\frac{\sqrt{\varepsilon^2+\Delta^2_{p,a}(T)\cdot f^2_{p,a}(x)}}{2\cdot k_B\cdot T}\right)}\right)\cdot dx}} \quad (10)$$

where subscripts *p*, *a*, ⊥, and ǁ designate polar, axial, perpendicular and parallel cases respectively. For this symmetry, the gap function is given by [22,25]:

$$\Delta(\widehat{\boldsymbol{k}},T) = \Delta(T)f(\widehat{\boldsymbol{k}},\widehat{\boldsymbol{l}}) \quad (11)$$

where, Δ(*T*) is the superconducting gap amplitude, ***k*** is the wave vector, and ***l*** is the gap axis. Thus, temperature dependence of λ(*T*) is determined by mutual orientation of the vector potential, ***A***, and the gap axis, ***l***, which is for transport current experiment just the orientation of the crystallographic axes of the film compared with the direction of the electric current.

There are two distinctive orientations, **A**⊥***l*** (when ***A*** is perpendicular to ***l***) and polar **A**||***l*** (when ***A*** is parallel to ***l***) [22,25]. More details can be found elsewhere [22,25,26]). The function of $w_{\perp,\parallel}(x)$ in Eq. 10 is:

$$w_{\perp}(x) = (1 - x^2)/2 \quad (12)$$

and

$$w_{\parallel}(x) = x^2 \quad (13)$$

and the gap amplitude in Eq. 11 is just Eq. 5, but η is given by [25]:

$$\eta_{p,a} = \frac{2}{3} \cdot \frac{1}{\int_0^1 f_{p,a}^2(x) \cdot dx} \quad (14)$$

where

$$f_p(x) = x \text{ ; polar configuration} \quad (15)$$

$$f_a(x) = \sqrt{1 - x^2} \text{ ; axial configuration} \quad (16)$$

More details about the $J_c(sf,T)$ analysis for *p*-wave symmetry can be found elsewhere [26,27].

By substituting Eqs. 5, 7-13 in Eq. 6, one can fit experimental $J_c(sf,T)$ data to *s*-, *d*-, *p*-wave gap symmetries to deduce λ(0), Δ(0), Δ*C*/*C*, T_c and $\frac{2\Delta(0)}{k_B T_c}$ as free-fitting parameters. This approach is recently applied for wide range of thin film unconventional superconductors [23,24,26-32].

III. $B_{c2}(T)$ analysis

There are several criteria to define $B_{c2}(T)$ from experimental *R*(*T*) curves. In this paper ti define $B_{c2}(T)$ we use the criterion of 3% of normal state resistance, $R_{norm}(T)$, for *R*(*T*) curves of $Nd_{0.8}Sr_{0.2}NiO_2$ presented in Fig. 4(a) by Li *et al* [3]. The fits of $B_{c2}(T)$ data to three models are shown in Fig. 1. It can be seen that ξ(0) values deduced by three models are close to each other and following analysis of $J_c(sf,T)$ will be utilized an average value of:

$$\xi(0) = 5.7 \pm 0.3 \; nm. \quad (17)$$

Preprints (www.preprints.org) | NOT PEER-REVIEWED | Posted: 15 December 2019 doi:10.20944/preprints201912.0191.v1

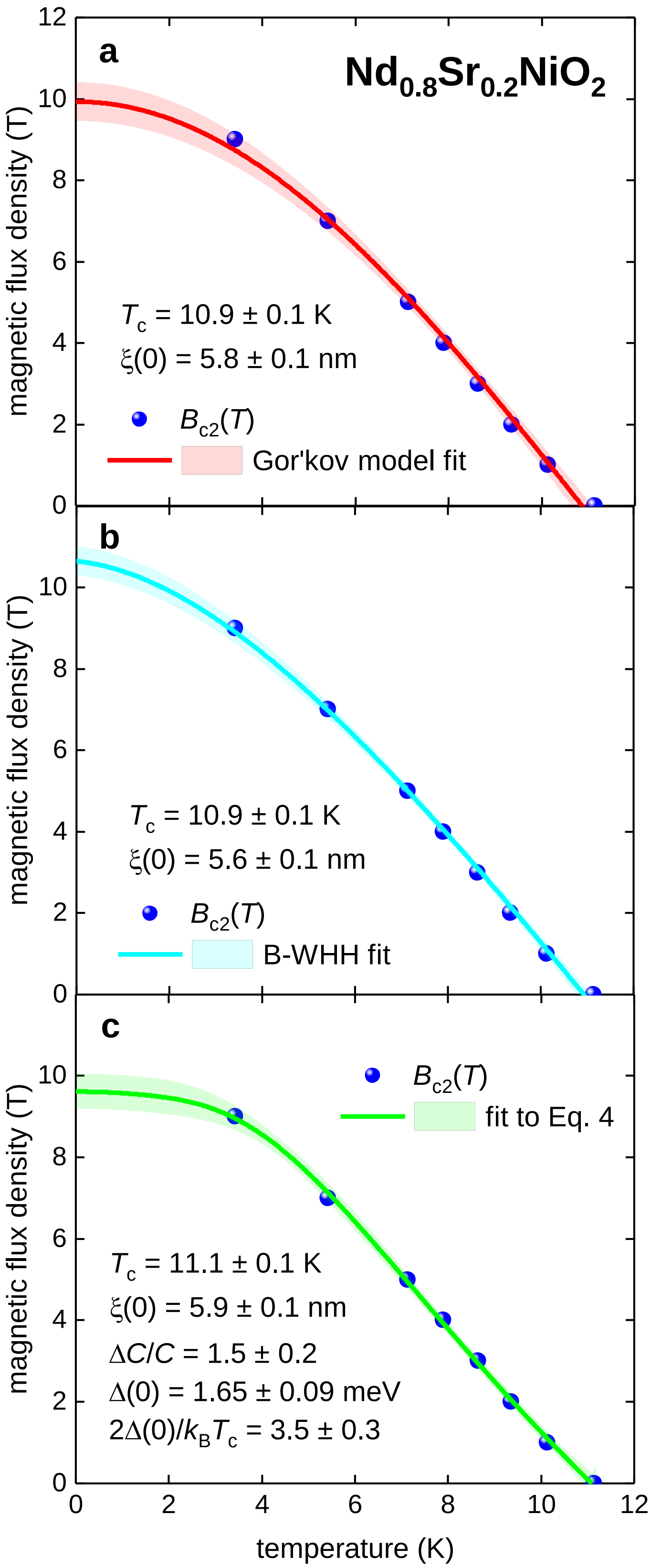

Figure 1. The upper critical field, $B_{c2}(T)$, of $Nd_{0.8}Sr_{0.2}NiO_2$ (reported by Li *et al* [3]) and data fits to three models (Eqs. 2-4). (a) fit to Gor'kov model, the fit quality is R = 0.995. (b) fit to B-WHH, R = 0.998. (c) fit to Eq. 4, R = 0.9993. 95% confidence bars are shown.

This deduced value for ξ(0) is in reasonable agreement with ξ(0) = 4.5 nm reported by Jovanović *et al.* [33] for copper-oxide-based infinite layer counterpart of $La_{1-x}Sr_xCuO_2$.

Deduced values by the fit to Eq. 4:

$$\frac{2\Delta(0)}{k_B T_c} = 3.5 \pm 0.3 \quad (18)$$

$$\frac{\Delta C}{C} = 1.5 \pm 0.2 \quad (19)$$

are, within uncertainties, equal to BCS [34] weak-coupling limits of 3.53 and 1.43 respectively, and the former deduced value is equal to recently deduced value of:

$$\frac{2\Delta(0)}{k_B T_c} = 3.51 \pm 0.05 \quad (20)$$

for *s*-wave oxide superconductor of $Ba_{0.51}K_{0.49}BiO_3$ [35].

It should be noted that there is no sign in experimental $B_{c2}(T)$ data that $Nd_{0.8}Sr_{0.2}NiO_2$ exhibits two superconducting band state, which can be seen as sharp enhancement in amplitude of $B_{c2}(T)$ at critical temperature of the second superconducting band opening (see for details Ref. 36).

IV. $J_c(sf,T)$ analysis

The critical current density, J_c, is defined as the lowest, detectable in experiment, value of electric power dissipation in a superconductor on electric current flow. For available $E(I)$ curves presented by Li *et al* [3] in their Fig. 3(f), the critical current density at self-field condition (when no external magnetic field is applied), $J_c(sf,T)$, can be defined at the lowest value of electric field of E_c = 3 V/cm. Experimental $J_c(sf,T)$ deduced by this E_c criterion and the fit to single band *s*-wave model (i.e., Eqs. 6,7 for which ξ(0) = 5.7 nm was fixed) are shown in Fig. 2(a). It can be seen that the fit is excellent, and deduced superconducting parameters (Fig. 2(a) and Table 1) are within BCS weak-coupling limits.

 doi:10.20944/preprints201912.0191.v1

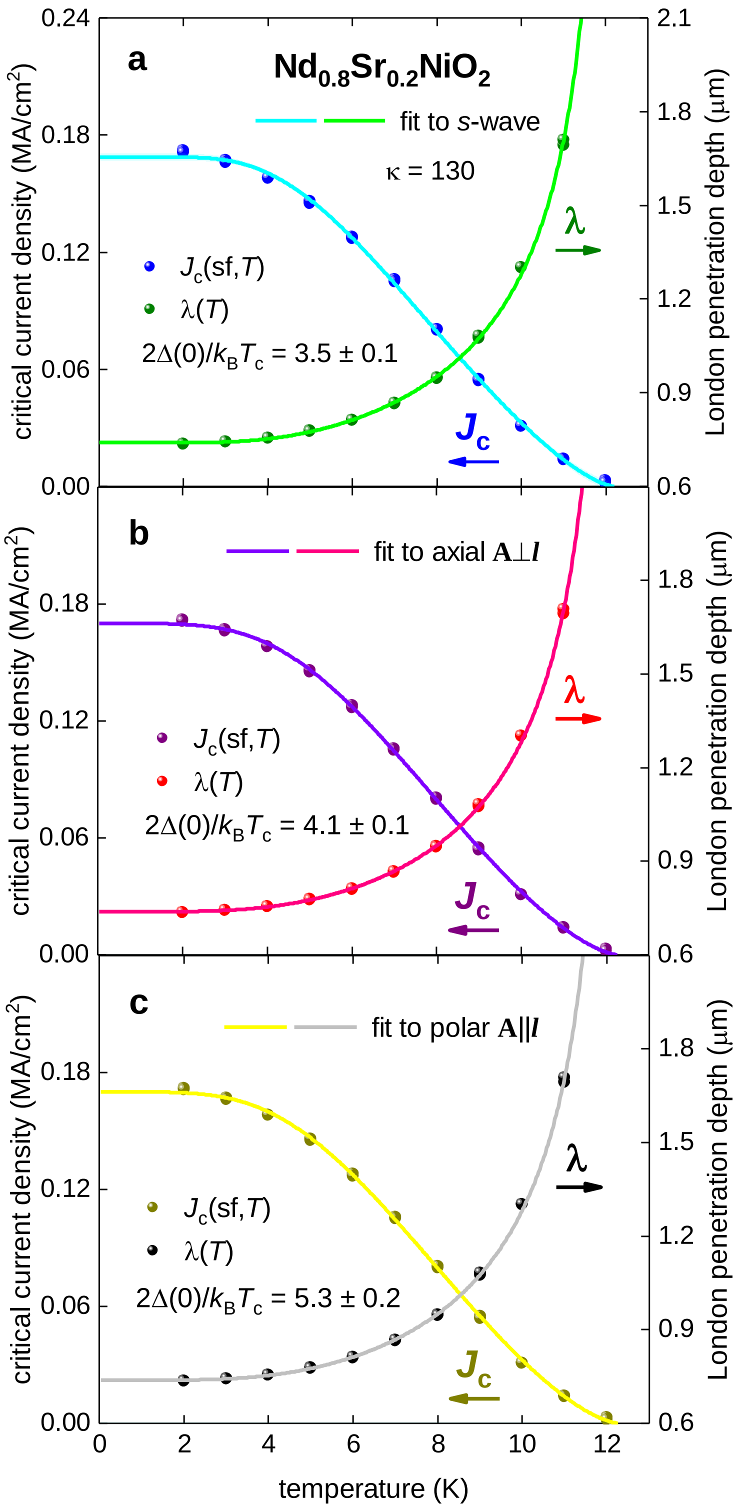

Figure 2. The self-field critical current density, $J_c(\mathrm{sf},T)$, for $Nd_{0.8}Sr_{0.2}NiO_2$ thin film with raw data processed from the work of Li *et al*. [3] and a fit of the data to three single-band models. For all models $\xi(0)$ = 5.7 nm was used. (a) *s*-wave fit, $\lambda(0) = 740 \pm 3$ nm, $T_c = 12.2 \pm 0.1$ K, the goodness of fit R = 0.995; (b) *p*-wave axial $\mathbf{A}\perp\boldsymbol{l}$ fit, $\lambda(0) = 738 \pm 2$ nm, $T_c = 12.3 \pm 0.1$ K, R = 0.997; (c) *p*-wave polar $\mathbf{A}\|\boldsymbol{l}$ fit, $\lambda(0) = 735 \pm 2$ nm, $T_c = 12.4 \pm 0.1$ K R = 0.9990. Other deduced parameters are listed in Table I.

Deduced λ(0) = 740 ± 3 nm is similar to λ(0) = 690-850 nm measured for samples possessing maximal T_c values for cuprate counterpart $La_{1-x}Sr_xCuO_2$ [37].

By utilizing deduced λ(0) value the Ginzburg-Landau parameter $\kappa = \frac{\lambda(0)}{\xi(0)} = 130$ which is similar to $La_{1-x}Sr_xCuO_2$ [33,37] and this value is at the upper-level range for other cuprates and unconventional superconductors [15,23,24,26,38-43].

Table I. Deduced $2\Delta(0)/k_BT_c$ and $\Delta C/C$ values for $Nd_{0.8}Sr_{0.2}NiO_2$ from $J_c(sf,T)$ fits to Eqs. 6-8 and BCS weak-coupling limits for the same parameters within for *s*-, *d*-, and *p*-wave pairing symmetries [20,23]. For *d*-wave symmetry, $\Delta_m(0)$ was used (which is the maximum amplitude of the *k*-dependent *d*-wave gap, $\Delta(\theta) = \Delta_m(0)\cos(2\theta)$).

Pairing symmetry and experiment geometry	Deduced $\frac{2\Delta(0)}{k_BT_c}$	BCS weak-coupling limit of $\frac{2\Delta(0)}{k_BT_c}$	Deduced $\frac{\Delta C}{C}$	BCS weak-coupling limit of $\frac{\Delta C}{C}$
s-wave	3.5 ± 0.2	3.53	1.5 ± 0.2	1.43
d-wave	> 10^2	4.28	2.3 ± 0.5	0.995
p-wave; axial **A**⊥***l***	4.1 ± 0.1	4.06	1.07 ± 0.08	1.19
p-wave; axial **A**‖***l***	9.0 ± 2.4	4.06	1.55 ± 0.05	1.19
p-wave; polar **A**⊥***l***	> $5\cdot10^2$	4.92	2.5 ± 0.4	0.79
p-wave; polar **A**‖***l***	5.3 ± 0.3	4.92	0.63 ± 0.03	0.79

Alternatively, *d*- and *p*-wave superconducting gap symmetries can be considered. The fits to *d*-wave symmetry, as well as to polar **A**⊥***l*** and axial **A**‖***l*** of *p*-wave, reveal very large $\frac{2\Delta(0)}{k_BT_c}$ values and these symmetries can be excluded from further consideration.

The cases of polar **A**‖***l*** and axial **A**⊥***l*** gap symmetries are still hypothetically possible (Table 1), and $J_c(sf,T)$ fit to these models are shown in Figs. 2(b,c) respectively, however, for given experimental conditions (i.e. epitaxial *c*-axis oriented thin film) expected geometry is polar **A**⊥***l*** [21].

It should be also noted that there is no sign for two-band superconductivity in $Nd_{0.8}Sr_{0.2}NiO_2$ which usually can be detected by a sharp enhancement in $J_c(sf,T)$ at critical temperature of the second band opening [24,36].

By taking in account a good agreement between $\frac{2\Delta(0)}{k_B T_c}$ and $\frac{\Delta C}{C}$ values deduced for *s*-wave symmetry from $B_{c2}(T)$ and $J_c(sf,T)$ analyses (Eqs. 17, 18 and Table 1, respectively), which are, in addition, within BCS weak-coupling limits for this symmetry, and a fact that *s*-wave pairing symmetry is the most conventional one, we can conclude that $Nd_{0.8}Sr_{0.2}NiO_2$ nickelate is weak-coupling single band high-κ *s*-wave superconductor.

V. Conclusions

Recently discovered [3] an infinite-layer nickelate $Nd_{0.8}Sr_{0.2}NiO_2$ superconductor is a new member of bulk oxide superconductors for which experimental $B_{c2}(T)$ and Jc(sf,T) data are analysed in this paper.

In result, it is found that an infinite-layer nickelate $Nd_{0.8}Sr_{0.2}NiO_2$ is weak-coupling single band high-κ *s*-wave superconductor.

Acknowledgement

Author thanks Dr. W. P. Crump (Aalto University) for invaluable help, and Prof. O. P. Sushkov (University of New South Wales), Prof. P. Bourges (Universite Paris-Sacray), and Prof. G. Seibold (Brandenburgische Technische Universität Cottbus–Senftenberg) for fruitful discussions.

Author also thanks financial support provided by the state assignment of Minobrnauki of Russia (theme "Pressure" No. AAAA-A18-118020190104-3) and by Act 211 Government of the Russian Federation, contract No. 02.A03.21.0006.

References

[1] Siegrist T, Zahurak S M, Murphy D W and Roth R S 1988 The parent structure of the layered high-temperature superconductors 1988 *Nature* **334** 231–232
[2] Azuma M, Hiroi Z, Takano M, Bando Y and Takeda Y 1992 Superconductivity at 110 K in the infinite-layer compound $(Sr_{1-x}Ca_x)_{1-y}CuO_2$ *Nature* **356** 775-776
[3] Li D, Lee K, Wang B Y, Osada M, Crossley S, Lee H R, Cui Y, Hikita Y and Hwang H Y 2019 Superconductivity in an infinite-layer nickelate *Nature* **572** 624-627
[4] Remeika J P, Geballe T H, Matthias B T, Cooper A S, Hull G W, Kelly E M 1967 Superconductivity in hexagonal tungsten bronzes *Physics Letters A* **24** 565-566
[5] Johnston D C, Prakash H, Zachariasen W H, Viswanathan R 1973 High temperature superconductivity in the LiTiO ternary system *Materials Research Bulletin* **8** 777-784
[6] Sleight A W, Gillson J L, Bierstedt P E 1975 High-temperature superconductivity in the $BaPb_{1-x}Bi_xO_3$ systems *Solid State Communications* **17** 27-28
[7] Bednorz J G and Müller K A 1986 Possible high Tc superconductivity in the Ba – La – Cu – O system *Zeitschrift für Physik B Condensed Matter* **64** 189-193
[8] Maeno Y, Hashimoto H, Yoshida K, Nishizaki S, Fujita T, Bednorz J G and Lichtenberg F 1994 Superconductivity in a layered perovskite without copper *Nature* **372** 532-534
[9] Hirsch J E, Marsiglio F 2019 Hole superconductivity in infinite-layer nickelates *Physica C* **566** 1353534
[10] Botana A S, Norman M R 2019 Similarities and differences between infinite-layer nickelates and cuprates and implications for superconductivity *arXiv*:1908.10946v2
[11] Jiang M, Berciu M, Sawatzky G A 2019 Doped holes in $NdNiO_2$ and high-T_c cuprates show little similarity *arXiv*:1909.02557
[12] Nomura Y, et al 2019 Formation of a two-dimensional single-component correlated electron system and band engineering in the nickelate superconductor $NdNiO_2$ *Phys. Rev. B* **100** 205138
[13] Li Q, He C, Si J, Zhu X, Zhang Y, Wen H-H 2019 Absence of superconductivity in bulk $Nd_{1-x}Sr_xNiO_2$ *arXiv*:1911.02420v3
[14] Ginzburg V L and Landau L D 1950 On the theory of superconductivity *Zh. Eksp. Teor. Fiz.* **20** 1064-1082
[15] Poole P P, Farach H A, Creswick R J, Prozorov R 2007 Superconductivity (2-nd Edition, London, UK)
[16] Gor'kov L P 1960 The critical supercooling field in superconductivity theory *Soviet Physics JETP* **10** 593-599
[17] Jones C K, Hulm J K, Chandrasekhar B S 1964 Upper critical field of solid solution alloys of the transition elements *Rev. Mod. Phys.* **36** 74-76
[18] Helfand E and Werthamer N R 1966 Temperature and purity dependence of the superconducting critical field, H_{c2}. II. *Phys. Rev.* **147** 288-294
[19] Werthamer N R, Helfand E and Hohenberg P C 1966 Temperature and purity dependence of the superconducting critical field, H_{c2}. III. Electron spin and spin-orbit effects *Phys. Rev.* **147** 295-302

[20] Baumgartner T, Eisterer M, Weber H W, Fluekiger R, Scheuerlein C, Bottura L 2014 Effects of neutron irradiation on pinning force scaling in state-of-the-art Nb_3Sn wires *Supercond. Sci. Technol.* **27** 015005
[21] Talantsev E F 2019 Classifying superconductivity in compressed H_3S *Modern Physics Letters B* **33** 1950195
[22] Gross F, Chandrasekhar B S, Einzel D, Andres K, Hirschfeld P J, Ott H R, Beuers J, Fisk Z, Smith J L 1986 Anomalous temperature dependence of the magnetic field penetration depth in superconducting UBe_3 *Z. Phys. B - Condensed Matter* **64** 175-188
[23] Talantsev E F 2018 Critical de Broglie wavelength in superconductors *Modern Physics Letters B* **32** 1850114
[24] Talantsev E F, Crump W P, Island J O, Xing Y, Sun Y, Wang J, Tallon J L 2017 On the origin of critical temperature enhancement in atomically thin superconductors *2D Materials* **4** 025072
[25] Gross-Alltag F, Chandrasekhar B S, Einzel D, Hirschfeld P J, Andres K 1991 London field penetration in heavy fermion superconductors *Z. Phys. B - Condensed Matter* **82** 243-255
[26] Talantsev E F, Iida K, Ohmura T, Matsumoto T, Crump W P, Strickland N M, Wimbush S C and Ikuta H 2019 *P*-wave superconductivity in iron-based superconductors *Scientific Reports* **9** 14245
[27] Talantsev E F, Mataira R C, Crump W P 2019 Classifying superconductivity in Classifying superconductivity in Moiré graphene superlattices *arXiv*:1902.07410v3
[28] Fête A, Rossi L, Augieri A and Senatore C 2016 Ionic liquid gating of ultra-thin $YBa_2Cu_3O_{7-x}$ films *Applied Physics Letters* **109** 192601
[29] Liu C, *et al.* 2018 Two-dimensional superconductivity and topological states in $PdTe_2$ thin films *Phys. Rev. Materials* **2** 094001
[30] Qu D-X, Teslich N E, Dai Z, Chapline G F, Schenkel T, Durham S R and Dubois J 2018 Onset of a two-dimensional superconducting phase in a topological-insulator–normal-metal $Bi_{1-x}Sb_x$/Pt junction fabricated by ion-beam techniques *Phys. Rev. Lett.* **121** 037001
[31] Pal B, *et al.* 2019 Experimental evidence of a very thin superconducting layer in epitaxial indium nitride *Supercond. Sci. Technol.* **32** 015009
[32] Zheliuk O, Lu J M, Chen Q H, El Yumin A A, Golightly S and Ye J T 2019 Josephson coupled Ising pairing induced in suspended MoS_2 bilayers by double-side ionic gating *Nature Nanotechnology* **14** 1123-1128
[33] Jovanović V P, Li Z Z, Raffy H, Briatico J, Sinchenko A A, Monceau P 2009 Resistive upper critical fields and anisotropy of an electron-doped infinite-layer cuprate *Physical Review B* **80** 024501
[34] Bardeen J, Cooper L N, Schrieffer J R 1957 Theory of superconductivity *Phys. Rev.* **108** 1175-1204
[35] Wen C H P, *et al.* 2018 Unveiling the superconducting mechanism of $Ba_{0.51}K_{0.49}BiO_3$ *Physical Review Letters* **121** 117002
[36] Talantsev E F 2019 Classifying induced superconductivity in atomically thin Dirac-cone materials *Condensed Matter* **4** 83
[37] Fruchter L, Jovanovic V, Raffy H, Labdi Sid, Bouquet F and Li Z Z 2010 Penetration depth of electron-doped infinite-layer $Sr_{0.88}La_{0.12}CuO_{2+x}$ thin films *Physical Review B* **82** 144529
[38] Puźniak R, Usami R, Isawa K, and Yamauchi H 1995 Superconducting-state thermodynamic parameters and anisotropy of $HgBa_2Ca_{n-1}Cu_nO_y$ by reversible magnetization measurements *Physical Review B* **52** 3756-3764

[39] Hosono H *et. al.* 2015 Exploration of new superconductors and functional materials, and fabrication of superconducting tapes and wires of iron pnictides *Sci. Technol. Adv. Mater.* **16** 033503
[40] Iida K, Hänisch J, and Tarantini C 2018 Fe-based superconducting thin films on metallic substrates: Growth, characteristics, and relevant properties *Applied Physics Reviews* **5** 031304
[41] Kauffmann-Weiss S *et al.* 2019 Microscopic origin of highly enhanced current carrying capabilities of thin NdFeAs(O,F) films *Nanoscale Advances* **1** 147 https://doi.org/10.1039/C9NA00147F
[42] Hänisch J *et al*. 2019 Fe-based superconducting thin films – Preparation and tuning of superconducting properties *Supercond. Sci. Technol.* **32** 093001
[43] Hosono H and Kuroki K 2015 Iron-based superconductors: Current status of materials and pairing mechanism *Physica C* **514** 399-422